Available online at www.sciencedirect.com
SCIENCE DIRECT®
Materials and Design 26 (2005) 41–46
Materials & Design
www.elsevier.com/locate/matdes

Friction stir welding of dissimilar Al 6013-T4 To X5CrNi18-10 stainless steel

Huseyin Uzun [a,*,1], Claudio Dalle Donne [a,1], Alberto Argagnotto [a,1], Tommaso Ghidini [a,1], Carla Gambaro [b]

[a] DLR-German Aerospace Center, Institute Materials Research, D-51170 Köln, Germany
[b] Università di Genova, Facoltà di Ingegneria, Italy

Received 2 December 2003; accepted 14 February 2004
Available online 15 June 2004

Abstract

The joining of dissimilar Al 6013-T4 alloy and X5CrNi18-10 stainless steel was carried out using friction stir welding (FSR) technique. The microstructure, hardness and fatigue properties of fiction stir welded 6013 aluminium alloy to stainless steel have been investigated. Optical microscopy was used to characterise the microstructures of the weld nugget, the heat affected zone (HAZ), thermo-mechanical affected zone (TMAZ) and the base materials. The results show that FSR can be used the joining of dissimilar Al 6013 alloy and X5CrNi18-10 stainless steel. Seven different zones of the microstructure in the welding are reported as follows: (1) parent stainless steel, (2) HAZ in the stainless steel at advancing side of weld, (3) TMAZ in the stainless steel at advancing side of weld, (4) weld nugget, (5) TMAZ in the Al alloy at retreating side of weld, (6) HAZ in the Al alloy at retreating side of weld and (7) parent Al alloy. A good correlation between the hardness distribution and the welding zones are observed. Fatigue properties of Al 6013-T4/X5CrNi18-10 stainless steel joints were found to be approximately 30% lower than that of the Al 6013-T6 alloy base metal.

Keywords: Friction stir welding; Dissimilar Al 6013/X5CrNi18-10; Stainless steel joint system; Microstructure; *S–N* curve

1. Introduction

Aluminium alloys with good heat transfer, high strength, good formability and weight saving are being considered for aerospace structure, shipbuilding, railway cars, etc. Stainless steel with excellent corrosion resistance, high static and dynamic strength, high toughness is a promising structural material in vehicle and aerospace applications. In order to achieve combine properties of aluminium alloys and stainless steel, development of reliable joints between Al-alloys and stainless steel is required to the considerable applications ranging from nuclear reactor components to domestic cooking utensils [1].

It is difficult to weld an Al-alloy to a stainless steel due to the large difference between their melting points. Recently, joints technology development of Al-alloys and stainless steel has been investigated for ultrasonic welding [2], explosive bonding [3], electric discharge bonding [4] and friction welding [5]. On the other hand, friction stir welding (FSW) is one of the most popular welding technique for joining dissimilar materials. FSW is a solid state process which is capable of generating reproducible high quality welds in similar aluminium alloys [6] and dissimilar materials, such as Cu/Al 6061 [7] and Al 6013/Al 2024 [8]. FSW has several advantages over the commonly used fusion welding methods, such as low energy input, short welding time, low distortion and relatively low welding temperatures. Therefore, FSW has been developed for aerospace, automotive, marine and nuclear assemblies. The joining takes place through the movement of a rotating shouldered tool with profiled pin

* Corresponding author. Present address: Department of Materials Technology, Faculty of Technology, Sakarya University, 54187 Esentepe, Sakarya, Turkey. Tel.: +90-264-346-02-69; fax: +90-264-346-02-62.
E-mail addresses: huzun@sakarya.edu.tr (H. Uzun), claudio.dalle-donne@dlr.de (C. Dalle Donne).
[1] Tel.: +49-02203-601-3571.

0261-3069/$ - see front matter © 2004 Elsevier Ltd. All rights reserved.
doi:10.1016/j.matdes.2004.04.002

plunged into the joint line between two pieces of sheet or plate material. When the rotating pin tool moves along the weld line, the material is heated up by the friction produced between the shoulder of the tool and the workpiece to be weld. Frictional heat causes the material to soften without reaching the melting point.

The objective of this paper, is to evaluate the joining of dissimilar Al 6013-T4 to X5CrNi18-10 by FSR. It is presented the welding zone microstructure in the friction welded dissimilar materials. It is also evaluated the microhardness changes on the welding zone and fatigue properties of Al 6013-T4 to X5CrNi18-10 joints. EDX analysis is performed to evaluate diffusion transition of elements between Al 6013-T4 alloy and stainless steel in the welding zone.

2. Experimental procedure

The 4 mm thick plates of 6013-T4 aluminium alloy and X5CrNi18-10 stainless steel were friction stir welded using an FSW adapted milling machine at DLR on the basic of the TWI procedure described in the patent [9]. The tool rotational speed and travel speed were 800 rpm and 80 mm/min, respectively. The welding direction of aluminium alloy was parallel to the rolling direction of the plate. Friction stir butt welding of dissimilar materials is schematically illustrated in Fig. 1. Unlike the conventional friction stir butt welding, the tool pin was shifted towards the aluminium plate. Therefore, the stirring action of the pin took part mainly in the aluminium. This was done to prevent an over heating of the aluminium. The chemical composition of the materials is given in Table 1.

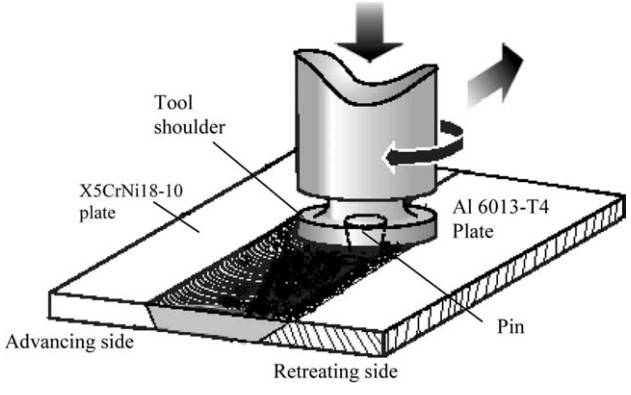

Fig. 1. Schematic views illustrating the friction stir welding of dissimilar Al 6013-T4 to stainless steel (X5CrNi18-10).

The Vickers microhardness tests were performed on the cross-section perpendicular to the welding direction using a 9.81N load for 30 s. The microstructure of the welding zone was observed by optical microscopy. The samples were polished using conventional polishing methods and etched. The determination of the level of diffusion elements in the welding zone between Al 6013 and base stainless steel and stainless steel particles in the weld nugget were analysed by scanning electron microscope equipped with an energy-dispersive X-ray spectroscopy (EDX) analysis system. The *S–N* fatigue testing was carried out on a 100 kN capacity resonance machine at constant load amplitude, constant stress ratio $R = 0.1$ and constant frequency of 62.5 Hz in laboratory air. The fatigue specimens having rectangular geometry were machined perpendicular to the weld line, with a gauge region 20 mm long, 9 mm wide and 2.5 mm thick. It should be kept in mind that the unstirred zone at the weld root, as can be seen in Fig. 2 within a circle, was machined to investigate the behaviour of dissimilar Al 6013 alloy to stainless steel joints without defect. Therefore this type of specimen, which is not reported in the ASTM specification, has just an experimental geometry.

3. Results and discussion

Fig. 2 shows a macroscopic overview of the cross-section of the friction stir welded dissimilar Al 6013 alloy to stainless steel. Unlike FSW in similar aluminium alloys [10], the dissimilar welds exhibit seven distinct regions, namely: (1) parent stainless steel, (2) heat affected zone (HAZ) in the stainless steel at advancing side of weld, (3) thermo-mechanically affected zone (TMAZ) in the stainless steel at advancing side of weld, (4) weld nugget, (5) TMAZ in the Al alloy at retreating side of weld, (6) HAZ in the Al alloy at retreating side of weld and (7) parent Al alloy. Optical micrographs of these regions indicated as "(a)–(h)" in Fig. 2 are shown in Fig. 3.

The base Al alloy contains elongated grains having diameter range of 80–120 μm in the rolling direction. The weld nugget exhibits a mixture of Al alloy and stainless steel particles pulled away by forge of tool pin from the stainless steel surface. Therefore the weld nugget has a composite structure of stainless steel particles reinforced Al 6013 alloy. Stainless steel particles have an irregular shape and inhomogeneous distribution within the weld nugget. Some of the particle especially coarse particles consist of microcrack because of high

Table 1
Chemical composition of Al 6013 alloy and X5CrNi18-10 stainless steel

Materials	Chemical compositions (wt%)									
	Cu	Mg	Mn	Fe	Si	Ni	Cr	Ti	Zn	C
Al 6013	1	0.9	0.5	0.3	0.8	–	0.1	0.1	0.1	–
X5CrNi18-10	–	–	1.45	Bal.	0.75	10	18	–	–	0.02

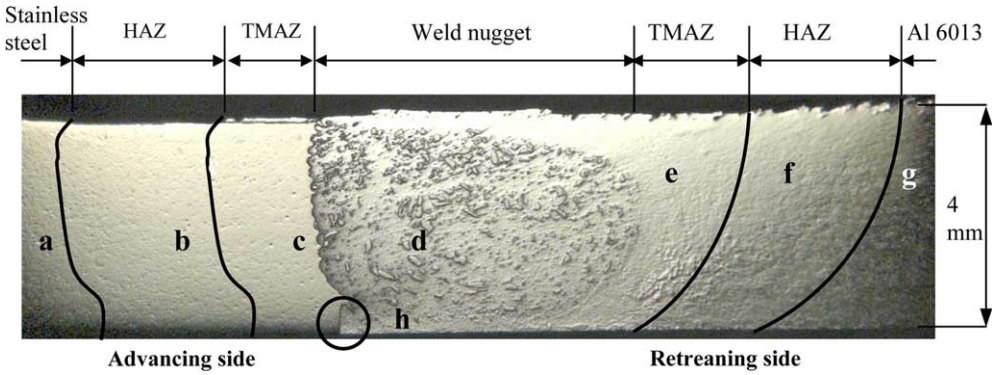

Fig. 2. Macroscopic overview of the cross-section of the friction stir welded Al 6013-T4 alloy to X5CrNi18-10 stainless steel.

deformation and intense mixture of materials as shown in Fig. 4. The Al alloy in the weld nugget consists of fine, equiaxed, recrystallized grains approximately 15 μm in size. The fine recrystallized grains in the stirred zone are attributed to the generation of high deformation and temperature during FSW.

A zone called TMAZ, which has been plastically deformed and thermally affected, is adjacent to the weld nugget at the retreating side. TMAZ is characterised by a rotation of up to 90° of the elongated grains of the base Al alloy. There is a heat affected zone (HAZ) between TMAZ and unaffected base Al alloy regions at the retreating side. The HAZ exhibits the same microstructure as the base Al 6013-T4 alloy.

The structure of base stainless steel shows typically coarse austenitic grains. The microstructure of the HAZ in the stainless steel at the advancing side nearly exhibits similar structure to the base stainless steel. The saw teeth appearance of the surface of stainless steel plate at the weld nugget interface is a direct consequence of the stirring action of the proprietary tool pin. The grains of stainless steel in the TMAZ at the advancing side are elongated through the teeth tips due to the high deformation.

The representative hardness profiles measured along the transverse cross section of the welded specimens at the centre, close to bottom and top of the welded region for the FSR of Al 6013-T4 alloy to stainless steel are indicated in Fig. 5. Almost the similar trend is observed in the hardness profiles among center, top and bottom lines. As can be seen from this figure, two different material properties of stainless steel and Al 6013 alloy exhibit two distinct hardness profiles of retreating (stainless steel side) and advancing (Al 6013 alloy side) sides. The hardness value at the retreating side sharply decreased towards the weld nugget from the level of TMAZ in the stainless steel at advancing side of weld. The weld nugget had an average hardness value of about 100 Hv, which is lower than that of the stainless steel base metal (200 Hv).

The hardness of the weld nugget having an inhomogeneous distribution of stainless steel particles depends on the measured point of the hardness indenter. Therefore the hardness of the weld nugget exhibits variable values due to the presence of the fine or coarse dispersed stainless steel particles in the weld nugget. The hardness value slightly decreases in the TMAZ at the advancing side (Al 6013 alloy side). The decrease in hardness in this zone is attributed to the second phase particle dissolution and coarsening caused by thermo-mechanical conditions. Also the dislocation density is low in this region, probably due to the dynamic recovery and recrystallization [11]. The minimum hardness is located around 6–11 mm from the weld centre at the retreating side. This hardness reduction is indicated to the HAZ in the Al 6013 alloy and characterised by the dissolution of all precipitates [12].

The slightly decrease in the hardness values in the HAZ of stainless steel at the advancing side indicates that there is no high enough temperature during the welding to take place microstructural changes. However the hardness increase in the upper zone of the weld is observed which could be attributed to the work hardening of the austenitic stainless steel.

The *S–N* curves for Al 6013-T4/stainless steel joint system obtained from fatigue test in the present study and Al 6013-T6 alloy [13] are shown in Fig. 6 for comparison purposes. Fatigue lifetimes of Al 6013-T4/stainless steel joints were found to be approximately 30% lower than that of the Al 6013-T6 alloy base metal. The specimen of friction stir welded Al 6013-T4 to stainless steel failed from cracks that had initiated on the root site of the welding zone where the lack of stirred material regions was found. Fig. 7 shows the crack initiation sites where the fatigue failure occurs. As can be seen from this Figure, failure surface exhibits a lack of stirred materials of Al 6013-T4 and stainless steel on the root of weld thus results of premature fatigue failure.

Fig. 8 shows macroscopic views of fatigue failure specimen. It is clear that the weld centreline does not coincide with the fatigue failure line. This indicates that the tool pin presumably moves towards the Al 6013-T4 alloy side during the welding and results lack of stirred materials. This had a detrimental effect on the decrease in the fatigue life of Al 6013-T4/satainless steel joint system.

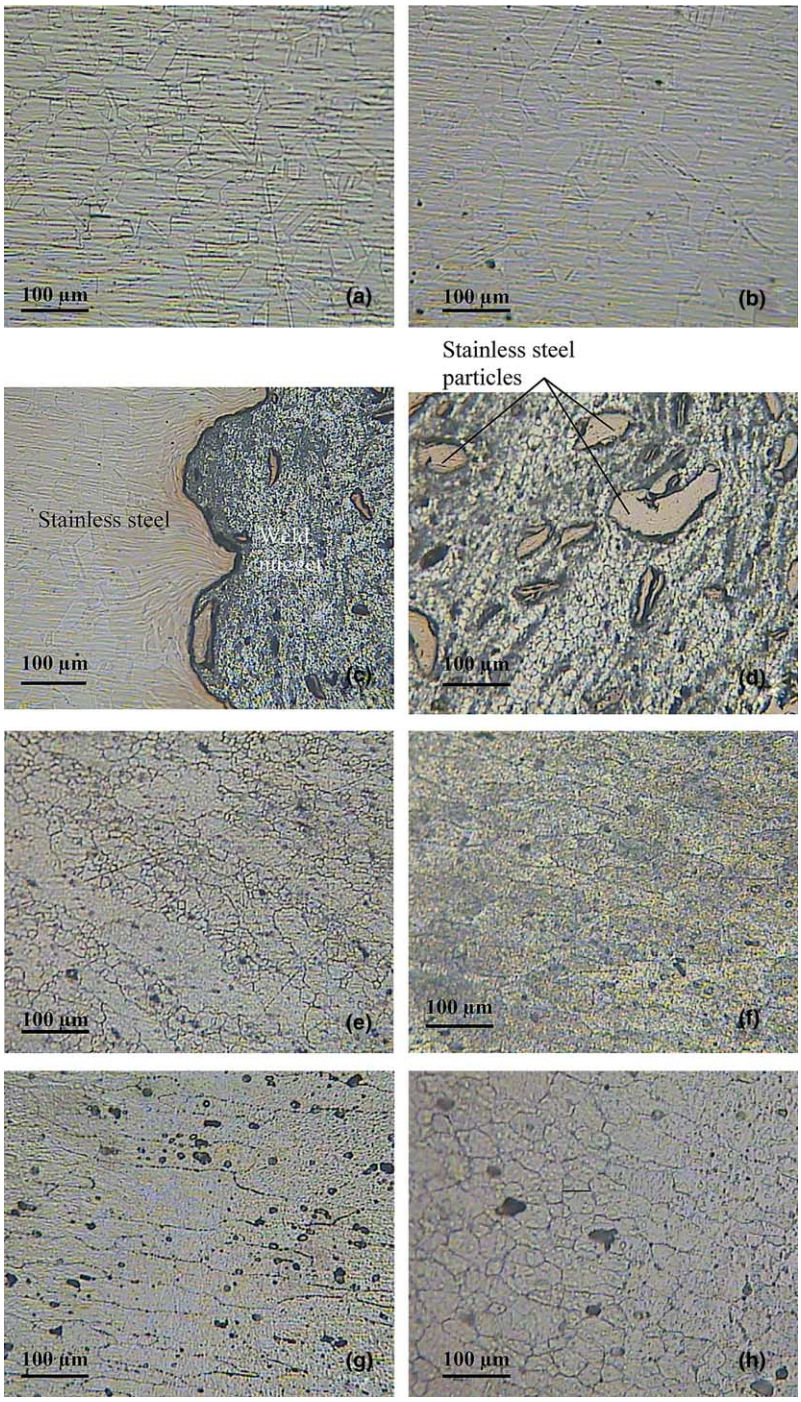

Fig. 3. Optical microstructures of the "(a)–(h)" regions shown in Fig. 2: (a) grain structure of base stainless steel, (b) HAZ at advancing side, (c) TMAZ at advancing side, (d) stainless steel particles surrounded by fine equiaxed grains of Al 6013 alloy in the weld nugget, (e) TMAZ at retreating side, (f) HAZ at retreating side, (g) base Al 6013 alloy and (h) grain structure of weld root.

Figs. 9 and 10 illustrate the representative concentration profiles of Cr, Ni, Fe and Al across the region of EDX analysis line (marked on the figures) at the interface between base stainless steel and Al 6013 alloy of weld nugget, and between stainless steel particles and Al 6013 alloy in the weld nugget, respectively. In fact, 50 points have been chosen across the region of analysis line with a counting time of minimum 50 s to get better statistics.

The concentration profiles of the elements at the interface between base stainless steel and Al 6013 alloy of weld nugget suggest that Al slightly diffuses in stainless steel, but Fe, Cr and Ni very little diffuse in Al 6013 alloy because of the sufficient temperature and time at the interface to diffuse the elements during the welding.

The diffuse transition between stainless steel particles and Al 6013 alloy in the weld nugget is not so

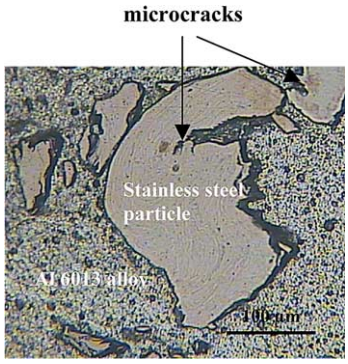

Fig. 4. Optical microstructure of weld nugget showing microcracks in the stainless steel particles.

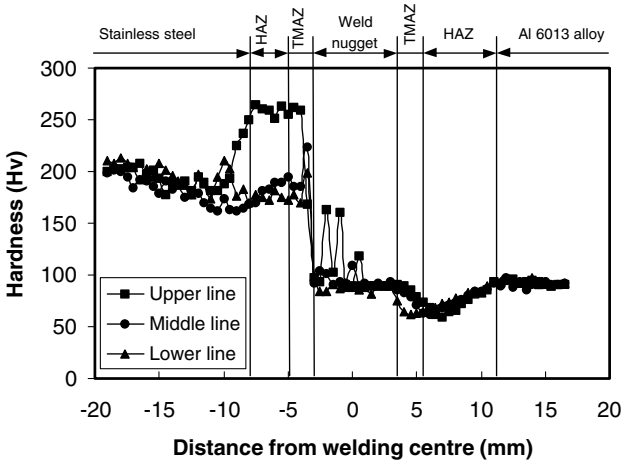

Fig. 5. The hardness profiles along the centre, upper and lower lines of the transverse cross-section.

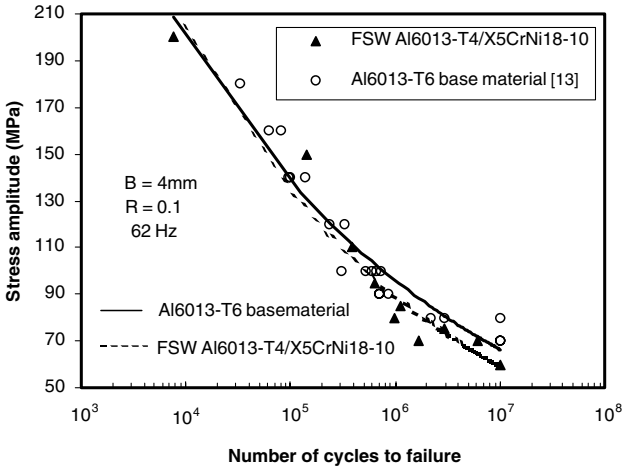

Fig. 6. *S–N* curves for Al 6013-T4/X5CrNi18-10 joint system and Al 6013-T6 base material.

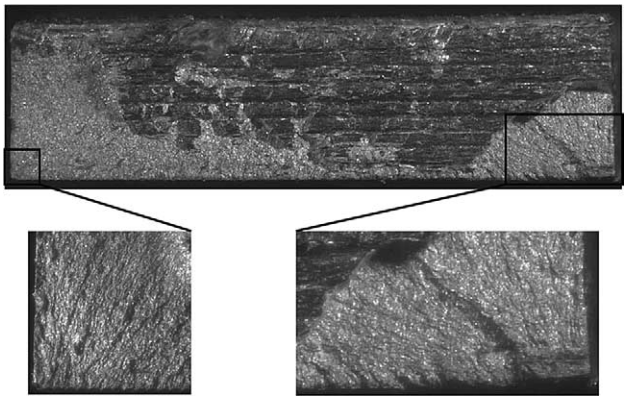

Fig. 7. The fatigue crack initiation sites.

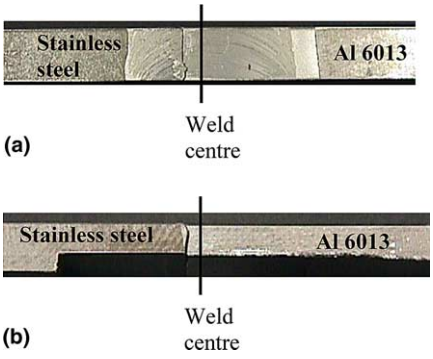

Fig. 8. Macroscopic views from: (a) top and (b) lateral of fatigue failured specimen.

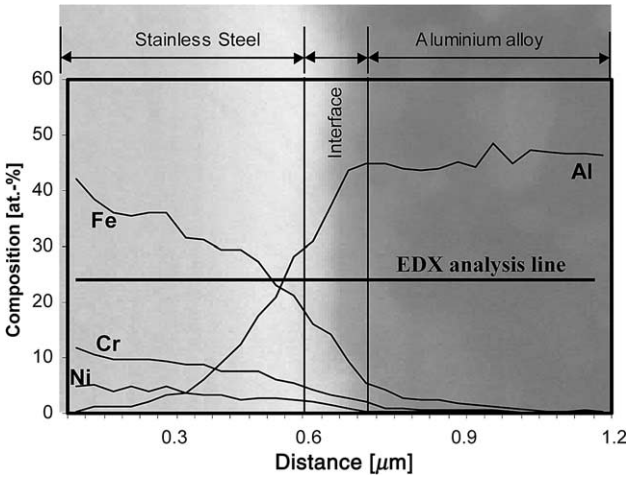

Fig. 9. Concentration profiles of Fe, Ni, Cr and Al across the region of EDX analysis line at the interface between base stainless steel and Al 6013 alloy of weld nugget.

pronounced. These concentration profiles indicate that while aluminium does not diffuse in stainless steel particles, Cr, Ni and Fe negligible diffuse in Al 6013 alloy in the weld nugget. These are attributed to the insufficient temperature, time and movement of particles in the weld nugget to diffuse the elements between stainless steel particles and Al 6013 alloy.

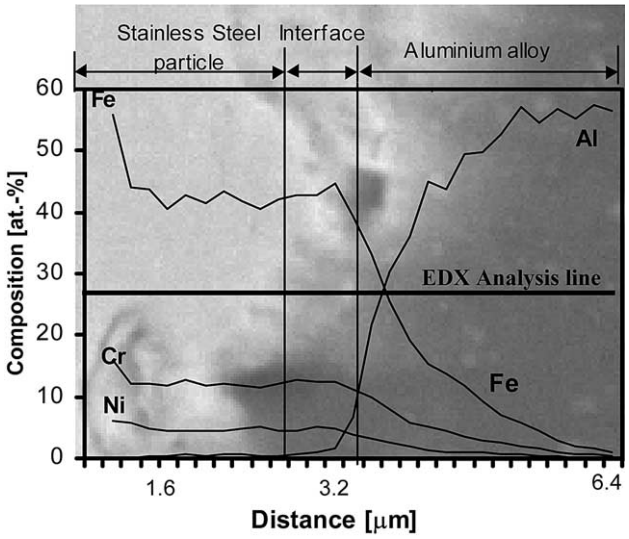

Fig. 10. Concentration profiles of Fe, Ni, Cr and Al across the region of EDX analysis line at the interface between stainless steel particles and Al 6013 alloy in the weld nugget.

4. Conclusions

A new welding technique, FSW, was succesfully applied to the joining of Al 6013 alloy and X5CrNi18-10 stainless steel. The microstructure, hardness, fatigue properties and EDX analysis of friction stir welded dissimilar Al 6013 alloy and stainless steel joints have been studied in the present work. Following conclusions are drawn: (1) The present study has demonstrated that Al 6013 alloy can be joined to dissimilar stainless steel using friction stir welding. (2) The microstructure of the welding zone in the friction stir welded dissimilar Al 6013 alloy to stainless steel was divided into seven zones: (1) parent stainless steel; (2) HAZ in the stainless steel at advancing side of weld; (3) TMAZ in the stainless steel at advancing side of weld; (4) weld nugget; (5) TMAZ in the Al alloy at retreating side of weld; (6) HAZ in the Al alloy at retreating side of weld; (7) parent Al alloy. (3) The hardness value at the retreating side sharply decreased towards the weld nugget from the level of the thermo-mechanically affected zone in the stainless steel at advancing side of weld. The hardness of the weld nugget shows variable values because of the presence of the fine or coarse dispersed stainless steel particles in he weld nugget. The hardness value slightly decreases in the TMAZ at the advancing side (Al 6013-T4 alloy side). The minimum hardness indicated to the HAZ in the Al 6013-T4 alloy is located around 6 to 11 mm from the weld centre at the retreating side. (4) Fatigue properties of Al 6013-T4/stainless steel joints were found to be approximately 30% lower than that of the Al 6013-T6 alloy base metal. (5) Aluminium slightly diffuses in stainless steel at the interface between base stainless steel and Al 6013 alloy of weld nugget, but Fe, Cr and Ni very little diffuse in Al 6013 alloy. The diffuse transition between stainless steel particles and Al 6013 alloy in the weld nugget is not so pronounced.

Further studies are needed to evaluate the effects of welding parameters of Al 6013/stainless steel system on the joining properties to establish the optimal weld parameters.

References

[1] Joining forces for multiple properties. Eureka February 2003 Available from: www.eurekamagazine.co.uk.
[2] Tsujino J, Hidai K, Hasegawa A, Kanai R, Matsuura H, Matsushima K, et al. Ultrasonic butt welding of aluminium, aluminium alloy and stainless steel plate specimens. Ultrasonics 2002;40:371–4.
[3] Kamachi Mudali U, Ananda Rao BM, Shanmugam K, Natarajan R, Raj B. Corrosion and microstructural aspects of dissimilar joints of titanium and type 304L stainless steel. J Nucl Mater 2003;321:40–8.
[4] Matsugi K, Wang Y, Hatayama T, Yanagisawa O, Syakagohri K. Application of electric discharge process in joining aluminium and stainless steel sheets. J Mater Process Technol 2003;135: 75–82.
[5] Lee WB, Yeon YM, Kim DU, Jung SB. Effect of friction welding parameters on mechanical and metallurgical properties of aluminium alloy 5052-A36 steel joint. Mater Sci Technol June 2003;19:773–8.
[6] Biallas G, Braun G, Dalle Donne C, Staniek G, Kaysser W. Mechanical properties and corrosion behaviour of friction stir welded 2024-T4. In: First International Symposium on Friction stir welding, TWI, 1999, cd-rom.
[7] Murr LE, Li Y, Flores RD, Trillo EA, McClure JC. Intercalation vortices and related microstructural features in the friction stir welding of dissimilar metals. Mat Res Innovat 1998;2:150–63.
[8] Dalle Donne C, Raimbeaux G. Residual stress effects on fatigue crack propagation in friction stir welds, In: International Conference on Fracture ICF 10, 3–7 December 2001, Hawaii, USA, Elesevier, NL, cd-rom.
[9] Thomas WM, Nicholas ED, Needham JC, Murch MG, Templesmith P, Dawes CJ. Improvements relating to friction welding. European Patent EP 0 615 480 B1; 1992.
[10] Lima EBF, Wegener J, Dalle Donne C, Goerigk G, Wroblewski T, Buslaps T, et al. Dependence of the microstructure, residual stresses and texture of AA 6013 friction stir welds on the welding process. Zeitschrift für Metallkunde (Int J Mater Res Adv Tech) 2003;94(8):908–15.
[11] Sato YS, Park SHC, Kokawa H. Microstructural factors governing hardness in friction stir welds of solid solution hardened Al alloys. Metal Mater Trans A 2001;32:3033–42.
[12] Juričić C, Dalle Donne C, Dreßler U. Effect of heat treatments on mechanical properties of friction stir welded 6013, In: Third International Symposium on Friction Stir Welding, Kobe, Japan, 27 and 28 September 2001, TWI (UK), cd-rom.
[13] Braun R, Biallas G, Dalle Donne C, Staniek G. Characterisation of mechanical properties and corrosion performance of friction stir welded AA6013 Sheet. In: Winkler PJ, editor. Materials for transportation industry EUROMAT'99. New York: Wiley VCH; 2000. p. 150–5.